GCAGS JOURNAL
A Publication of the Gulf Coast Association of Geological Societies
www.gcags.org

Maximizing Value from Drill Cuttings: A Case Study in the Eagle Ford Using Robotic XRF Logging

David Tonner and Andreina Liborius

Diversified Well Logging, 9780 Pozos Ln., Conroe, Texas 77303, U.S.A.

ABSTRACT

Drill cuttings, often overlooked for their potential value, are a free byproduct of drilling operations. This case study unveils a series of cutting-edge, innovative techniques that extract maximum value from drill cuttings in the Eagle Ford Shale of South Texas. These techniques, developed to tackle the area's renowned geological complexity, with lateral facies changes and subseismic scale faulting, are a significant leap forward in the industry. These conditions present significant challenges for standard measurement while drilling (MWD) and gamma-ray (GR) tools, which often fall short of sufficient information for decision-making. Whereas complex logging while drilling (LWD) tools are helpful, they come at a high cost and carry significant risks.

By employing an innovative automated sampling system with quantitative X–ray fluorescence (XRF) and laser-induced breakdown spectroscopy (LIBS), we can analyze 11 major oxides and 33 trace elements. This cutting-edge process generates a surface GR from uranium, potassium, and thorium summation. This surface GR measurement is a promising, low-cost, high-tech alternative to traditional tools. In a study spanning over two years using 80 wells, we introduced robotics for automated sample collection, which significantly lowered health, safety, and environmental (HSE) risks, improved sample collection frequency, reduced human error, and allowed personnel to focus on value-added tasks. This approach mitigated MWD tool failures and significantly enhanced geosteering operations, optimizing well placement and increasing reservoir contact. The benefits of these new techniques are not just theoretical but have been proven in practice, offering a promising future for drilling efficiency and resource utilization.

INTRODUCTION

The Eagle Ford Shale, a significant hydrocarbon-producing formation in Texas, is a key player in the oil and gas industry. It spans across the state from the Mexican border into East Texas, roughly 50 miles wide and 400 miles long, with an average thickness of 250 feet (see Figure 1). This drilling environment, with unique challenges such as high temperatures of around 200 to 250 degrees Fahrenheit and significant geological complexity, including lateral facies changes and subseismic scale faulting, necessitates innovative solutions (see Figure 2). The unique challenges of the Eagle Ford Shale, such as its high temperatures and complex geological structures, underline the need for innovative drilling techniques. Standard measurement while drilling (MWD) and gamma-ray (GR) tools often fall short in these conditions, and whereas MWD tools offer improved subsurface understanding, they are expensive and come with risks. MWD tools are complex and contain sensitive electronic components that can fail under harsh downhole conditions, such as high temperature and pressure. Tool failure can lead to non-productive time (NPT), which increases operational costs. MWD tools can become stuck in the wellbore or be lost due to wellbore instability, differential sticking, or tool string failure. Retrieving lost tools can be costly and time-consuming, and in some cases, the tools may need to be retrievable, resulting in financial loss. MWD tools may not always provide accurate or reliable data, especially in complex geological settings or under challenging downhole conditions. Data quality can be affected by tool calibration, formation properties, or environmental interference (e.g., noise from other equipment). MWD tools can lead to safety hazards, such as leaks of radioactive sources (if used) or electrical shorts that could pose a risk to personnel and the environment. This study uses an automated sampling system with quantitative X–ray fluorescence (XRF) and laser measurements of drill cuttings to provide a surface GR as an alternative to traditional downhole measurements. The aim is to address these geological and drilling challenges, reduce costs, enhance drilling efficiency, improve operational safety, and provide critical geological insights such as staying within landing zones and understanding facies change and complex structures.

The Eagle Ford was deposited in various depositional environments ranging from open marine conditions in the southwest to more restricted settings in the northeast (Hentz and Ruppel, 2010; Donovan et al., 2015) (Fig. 3). This variability

Manuscript received August 8, 2024; revised manuscript received June 27, 2025; manuscript accepted July 8, 2025.

GCAGS Journal, v. 14 (2025), p. 59–75.
https://doi.org/10.62371/TXQB8591

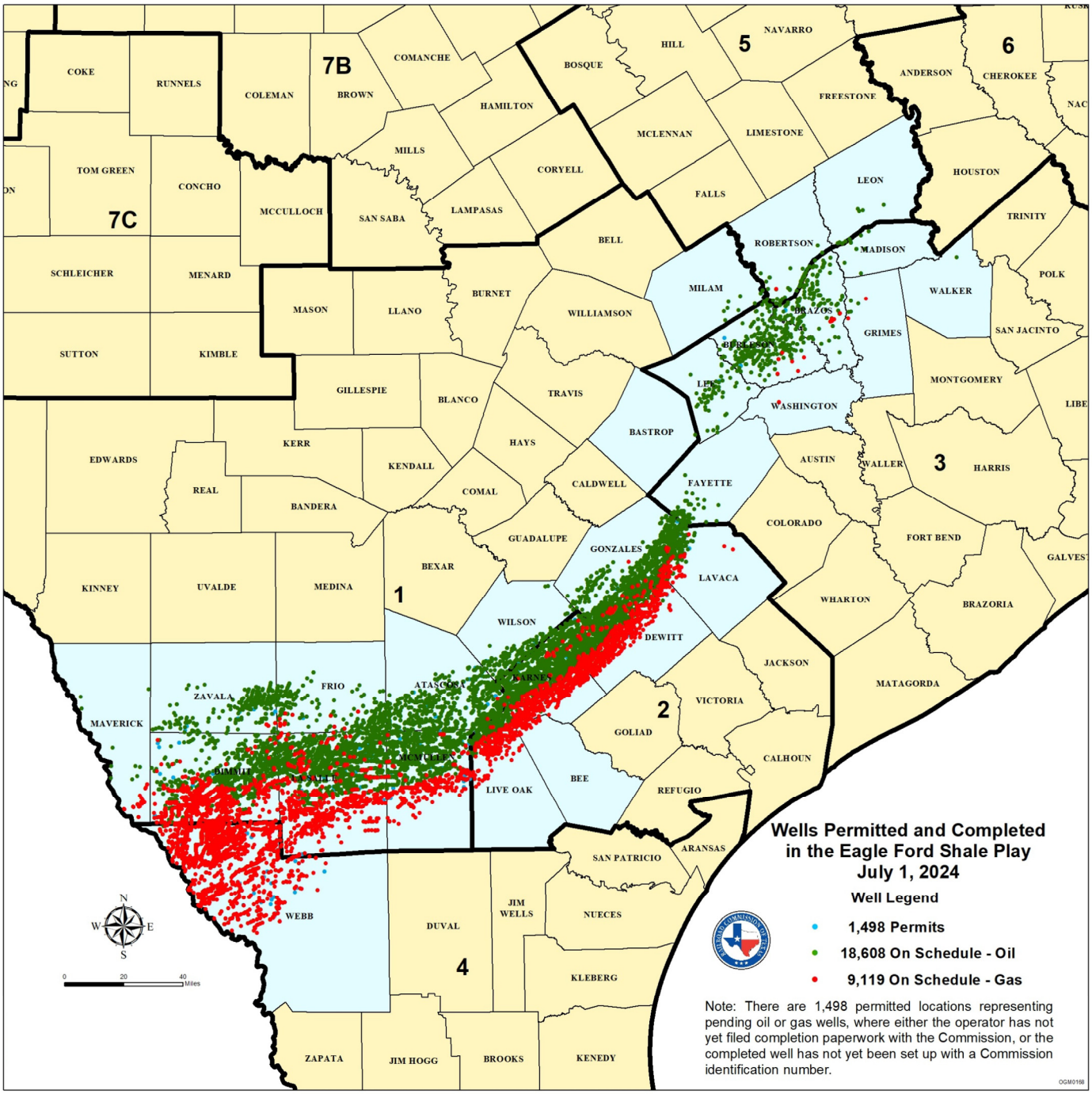

Figure 1. Map of Eagle Ford Shale drill locations, South Texas. Adapted from the Railroad Commission of Texas (2024).

resulted in significant lateral changes in lithology, organic content, and reservoir properties across the formation. In the southwest, near the Mexican border, the Eagle Ford is thicker and more carbonate-rich. This area is characterized by high levels of organic material and greater deposition of carbonate muds, leading to the formation of calcareous shales. The high organic content and carbonate nature of the rock make it a significant source rock with excellent hydrocarbon potential. The depositional environment here was more influenced by open marine conditions, with higher energy settings that led to the formation of thicker, more continuous beds. The abundance of organic matter suggests that this region experienced more anoxic conditions favorable for hydrocarbon preservation. Moving northeast, the Eagle Ford becomes thinner and more siliciclastic (rich in silica, such as quartz). This area exhibits a higher proportion of siltstones and sandstones interbedded with shales. The northeast section of the Eagle Ford was deposited in a more restricted marine environment, closer to the shoreline. This setting led to more frequent interruptions in sedimentation, contributing to its heterogeneous nature. In this region, the depositional energy was lower, and the environment was influenced by terrigenous input, which increased the amount of siliciclastic material. As a result, the northeast Eagle Ford contains more clay-rich shales and siltstones, and the organic content is typically lower than in the southwest. (Hentz and Ruppel, 2010; Donovan et al., 2015) (see Figure 4).

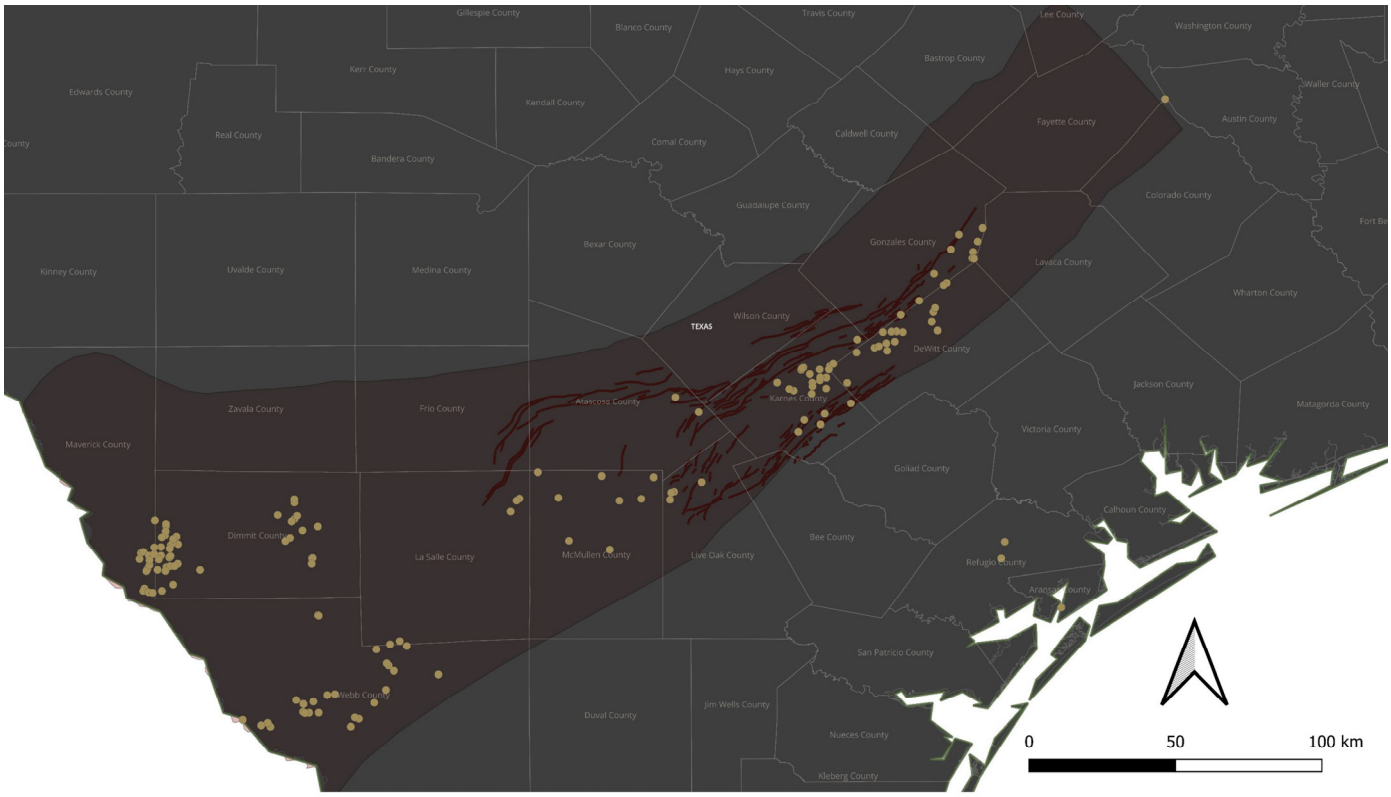

Figure 2. Eagle Ford XRF database.

AUTOMATED XRF DATA COLLECTION AND UTILIZATION

The theory underpinning this approach involves the analysis of drill cuttings using XRF to detect 11 major oxides and 33 trace elements ranging from Mg to U. Gamma radiation emitted by elements such as K, Th, and U and their decay products (ground-based radiation) exists at trace levels in all subsurface formations. It represents the primary external source of irradiation. Based on this principle, the output is field records with mineralogy, lithology, and elementary GR based on gamma radiation emitted by U. Th, and K ($16K_2O + 8U + 4Th$) (Ellis and Singer, 2007), guaranteeing the sampling quality. This data is beneficial (because it allows an elementary GR record in API units), especially when the logging while drilling [LWD] tools fail, avoiding the need to rerun tools leading to NPT. The higher the sampling density in the well, the greater the tool's utility as it approaches the depth resolution of a GR LWD log.

The primary challenges include ensuring the accuracy and reliability of surface GR data and integrating robotic systems to streamline sample collection processes. Anoxic proxies such as Mo, V, Ni, Cu, Co, and U are well-established indicators in geochemical analysis for interpreting redox conditions, particularly in source rock studies (Algeo and Tribovillard, 2009; Tribovillard et al., 2006). Heavy elements like Ti, Zr, Rb, and Nb, along with elemental ratios such as Ni/Mo, Zn/Mo, and Rb/Zr, provide critical insights into depositional environments, diagenesis, and sediment provenance (Hild and Brumsack, 1998; Reimann et al., 2011). In the context of the Eagle Ford Shale, these geochemical indicators are valuable for reconstructing depositional settings and optimizing well placement (Romero-Sarmiento et al., 2014; Liu et al., 2017).

The Ni/Mo ratio, for instance, is widely used as a proxy for reducing conditions during deposition; higher values often reflect more reducing environments favorable for organic matter preservation (Algeo and Maynard, 2004). This is particularly relevant for identifying organic-rich zones within the Eagle Ford Shale with greater hydrocarbon generation potential (Romero-Sarmiento et al., 2014). Zn/Mo ratios have also been applied in this context to refine interpretations of paleo-redox conditions (Hild and Brumsack, 1998). The Rb/Zr ratio serves as a proxy for sediment provenance and detrital input, with Rb typically associated with clay minerals and Zr with resistant siliceous grains such as zircon. A high Rb/Zr ratio suggests a predominance of fine-grained, distal sediments, indicative of low-energy, deep marine settings, whereas a low ratio may reflect coarser, more proximal inputs (Reimann et al., 2011; Liu et al., 2017). In the Eagle Ford Shale, such variations in the Rb/Zr ratio can aid in distinguishing sedimentary facies and predicting mechanical behavior relevant to hydraulic fracturing efficiency.

Figure 5 is a detailed geochemical and stratigraphic analysis using XRF data. The XRF data, collected at 6 inch intervals over the core, highlights the high-resolution nature of this data collection. Sampling at 6 inch intervals enables detailed mapping of geochemical variations within the core, crucial for identifying subtle changes in mineralogy and geochemistry. Such details can provide insights into depositional environments, diagenetic processes, and hydrocarbon potential.

The results from the XRF data analysis are consistent with existing geological studies, supporting the credibility of the data and methods used. This alignment suggests that the stratigraphic and geochemical interpretations are robust and align with the broader geological understanding of the region (Larson et al., 2023; Tinnin et al., 2016).

The chart includes various stratigraphic columns with geochemical ratios such as Ni/Mo and Rb/Zr, which are used to interpret organic richness, redox conditions, and sedimentary processes. These columns interpret geological features such as organic richness, redox conditions, and sedimentary processes. These ratios provide insights into paleoenvironmental conditions,

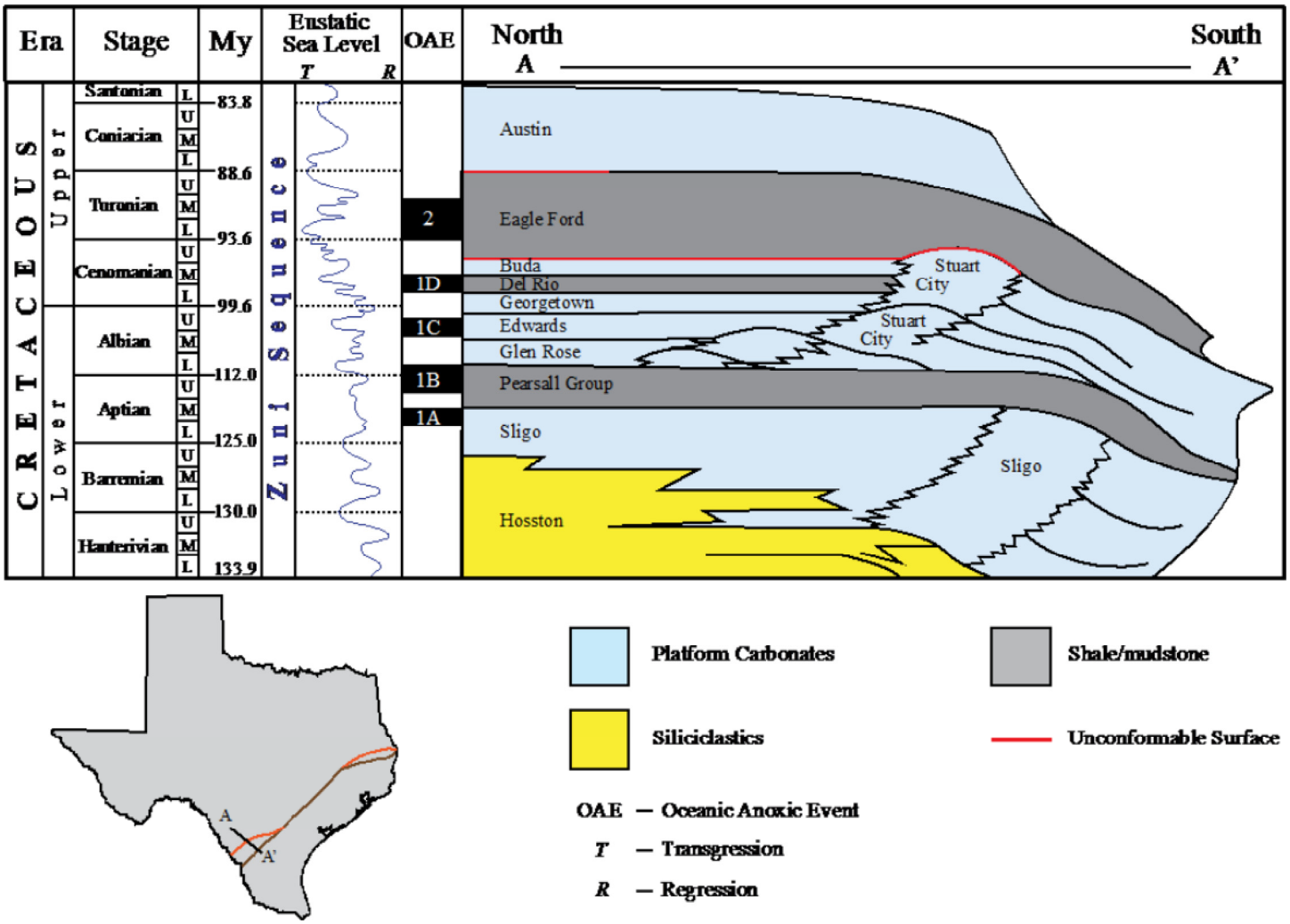

Figure 3. Diagrammatic representation of the evolution and architecture of Cretaceous carbonate platforms (adapted from Workman et al. [2013]). The figure summarizes the Cretaceous transgression-regression cycles of the Zuni Sea. The Comanche Shelf consists of alternating platform carbonates and organic-rich carbonate muds. Organic-rich mudstones coincide with global oceanic anoxic events (OAEs), representing platform inundation and drowning episodes. These episodes define periods of open-shelf and rimmed-shelf architectures.

essential for understanding the potential for hydrocarbon generation and preservation.

OAE 2 (oceanic anoxic event 2) is noted and serves as a key stratigraphic marker associated with periods of widespread anoxia, which can lead to the preservation of organic matter and thus be of interest for hydrocarbon exploration. Identifying such markers in the core can provide valuable information about the timing and extent of anoxic conditions in the depositional environment.

Color-coding and patterns in the chart relate to chemostratigraphic units and geochemical data, making it easier to interpret complex data sets. This ground truth information provides context for interpreting the drill cuttings XRF data on subsequent wells.

DESCRIPTION AND APPLICATION OF EQUIPMENT AND PROCESSES

Quantitative XRF analysis was conducted on drill cuttings to measure the concentrations of major oxides and trace elements. Advanced XRF analyzers and robotic systems were utilized to automate sample collection boxes near the shale shaker and the collection center for laser analysis (see Figure 6).

The robotic system is a testament to the commitment to safety. The system collected drill cuttings regularly, significantly reducing human error, improving sample collection frequency, and lowering health, safety, and environmental (HSE) risks. The XRF and laser analysis were performed on-site, with the surface GR data compared to standard downhole GR data to validate its depth accuracy. Integrating robotics requires careful calibration and coordination with existing drilling operations to ensure seamless functionality. A proprietary extraction device employing a motive base fluid was used. Using a motive fluid, such as water, diesel, or another compatible fluid, is essential for the functionality of this system. The motive fluid is pumped at high speed through a tube of varying diameters. As it accelerates through the narrow constriction, it generates a low-pressure area. This low-pressure zone creates a suction force that pulls drill cuttings or fluid samples from the surrounding environment, such as the drilling mud or slurry near the wellbore, into the system. This process ensures continuous and efficient extraction of samples, even from high-flow-rate environments or those with varying

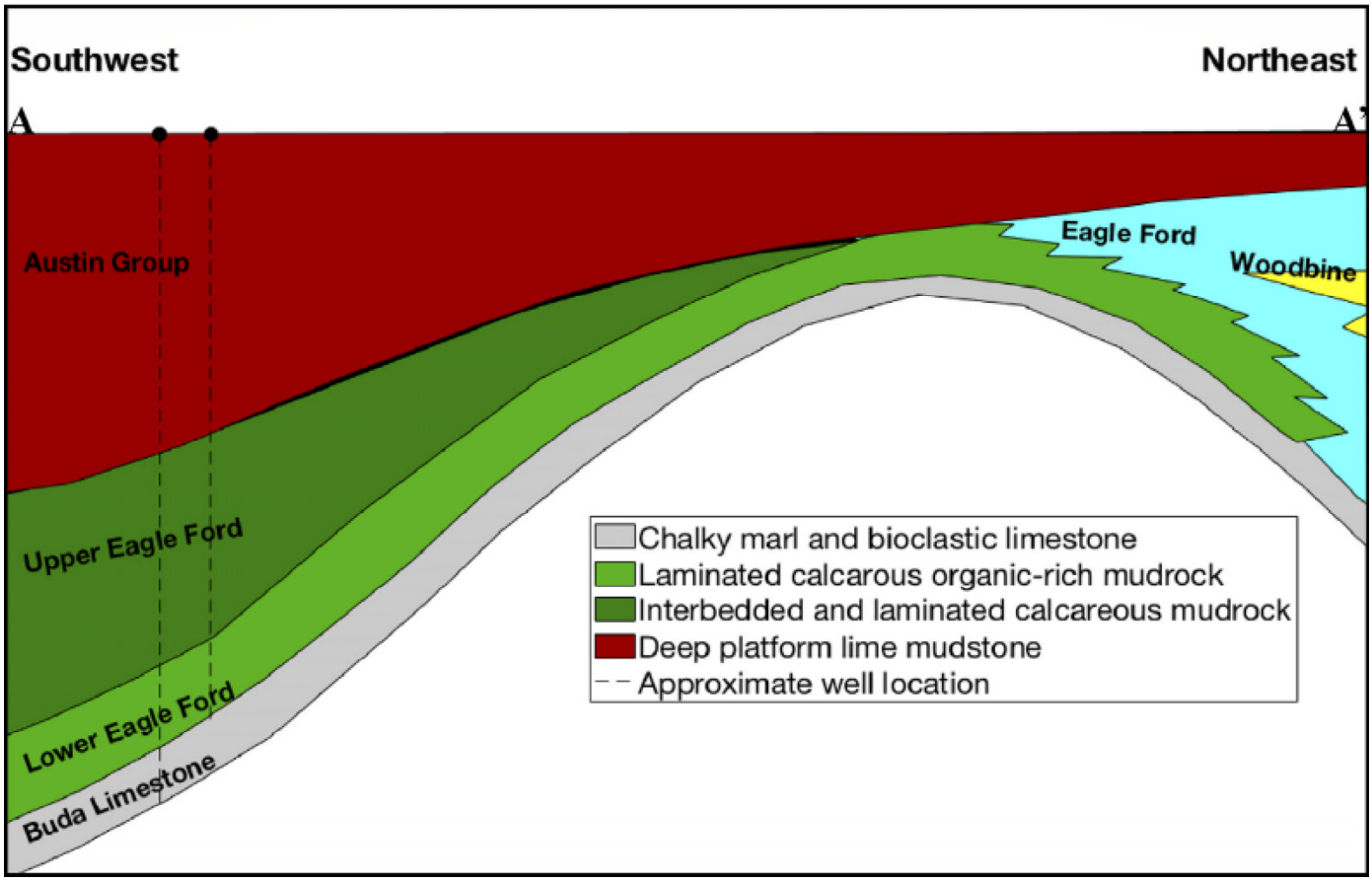

Figure 4. Main stratigraphic groups and formations in the study area (not to scale) (modified after Amosu [2015]).

pressures. Positioned 30 to 60 feet from the collection center, this device utilized the motive fluid to transport and clean the drill cuttings as they traveled from the header box.

Data quality assurance and quality control (QAQC) was conducted continuously, 24/7. Elemental GR (EGR) was calculated and compared to the MWD GR downhole data to ensure the depth representativity of the cuttings (Fig. 7). Discrepancies indicated potential issues with GR calibration, hole cleaning, wellbore stability, wellbore tortuosity, or sample collection and processing. A quality flag system confirmed that the cuttings were representative and on depth. Additionally, the levels of barium contamination, a major component of drilling mud, were measured. Values exceeding 10,000 ppm indicated improper washing of samples, as high barium levels suggest inadequate cuttings cleaning. Thirdly, a global reference standard of known composition was run through the machine for every 5th sample to ensure the highest level of data quality and verify that the instrument response was not drifting.

A data-driven approach incorporating machine learning and artificial intelligence (AI) was employed. Initially, unsupervised hierarchical clustering analysis (HCA) and principal component analysis (PCA) were applied to the Austin Chalk, Upper Eagle Ford (UEF), and Lower Eagle Ford (LEF) formations using previously collected elemental data from DeWitt County. These methods follow the general frameworks described by Everitt et al. (2011) for HCA and Jolliffe (2002) for PCA. PCA analysis established 5 chemostratigraphic zonations for AC/UEF/LEF (Fig. 8).

PCA and clustering are powerful statistical methods to analyze complex datasets, such as inorganic chemical elemental data, to identify depositional environments. PCA reduces the complexity of the data by transforming it into principal components that capture the most significant variations. The process begins with data standardization to ensure that each variable, or element concentration, contributes equally to the analysis. Next, PCA identifies principal components, which are combinations of elemental variables like Si, Al, and Mg that represent major patterns of variation in the data. These components are then interpreted to infer depositional environments. For instance, a principal component dominated by Ca and Mg might suggest a marine carbonate environment.

Carbonate facies are sedimentary environments dominated by carbonate minerals, such as limestone and dolomite, typically found in shallow, warm marine settings like reefs, lagoons, and continental shelves. These facies form from the accumulation of carbonate sediments produced by marine organisms, such as corals and shellfish. Key indicators of carbonate facies include high levels of Ca and Mg, essential for forming carbonate minerals. Sr is also common, indicating the presence of aragonite. These facies often show features like crossbedding and fossils, reflecting high-energy environments and active biological processes. Carbonate facies are significant for reconstructing past marine conditions and serve as important reservoirs for hydrocarbons due to their porosity and permeability.

Detrital facies, formed from sediments transported and deposited by physical processes such as rivers, wind, or glaciers, can be identified by analyzing specific elements. Si is a key indicator, as it is a major component of quartz, commonly found in siliceous detrital sediments like sandstones and siltstones. Al is another important element, often present in clay minerals and

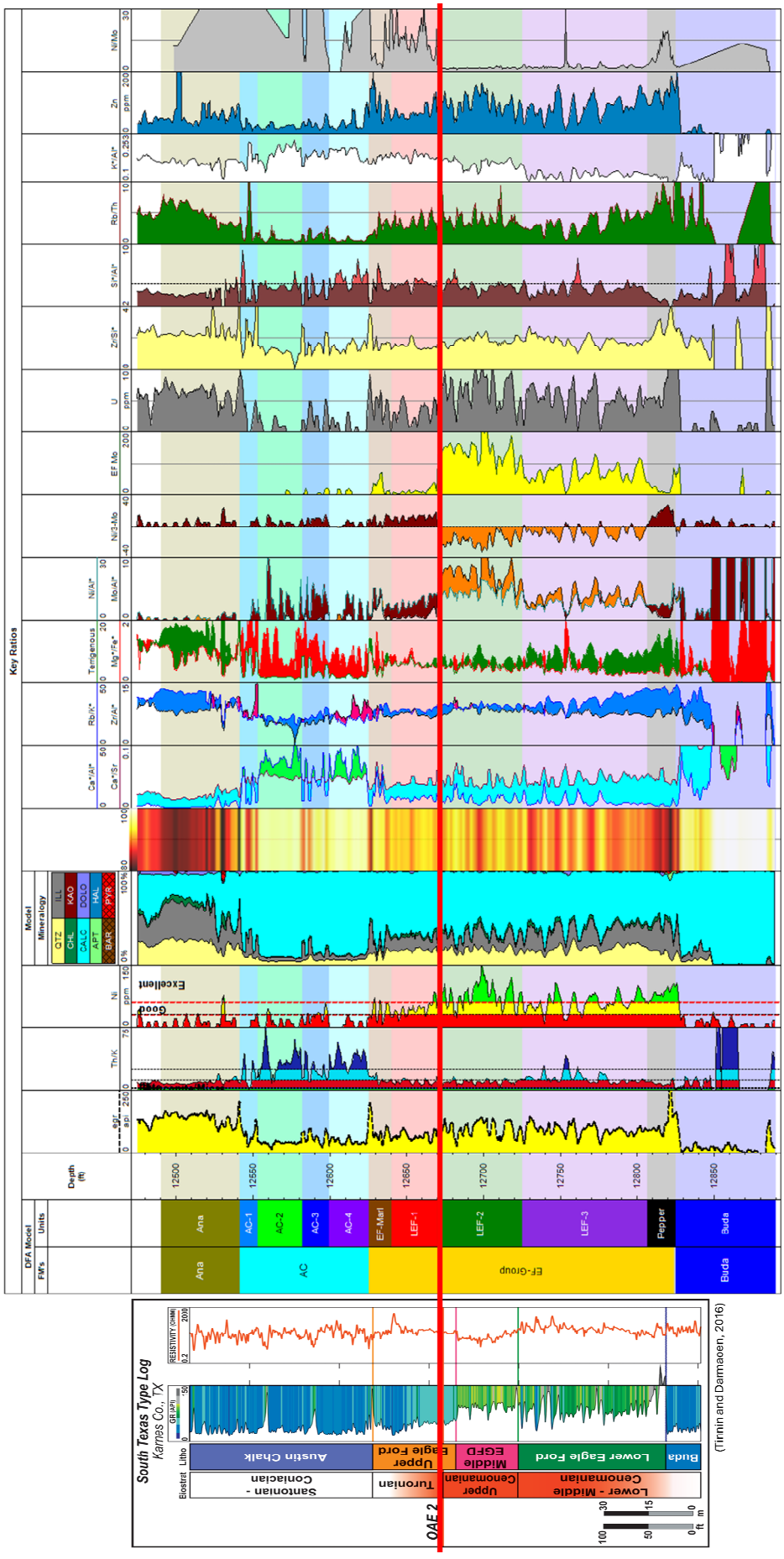

Figure 5. XRF data calibration at 6 inch intervals over a core from the Eagle Ford Shale. The XRF data correlates well with geological literature, highlighting key stratigraphic markers like oceanic anoxic events (OAE 2). Elemental ratios such as Ni/Mo and Rb/Zr provide insights into redox conditions and sediment provenance, supporting well placement optimization and geological interpretation.

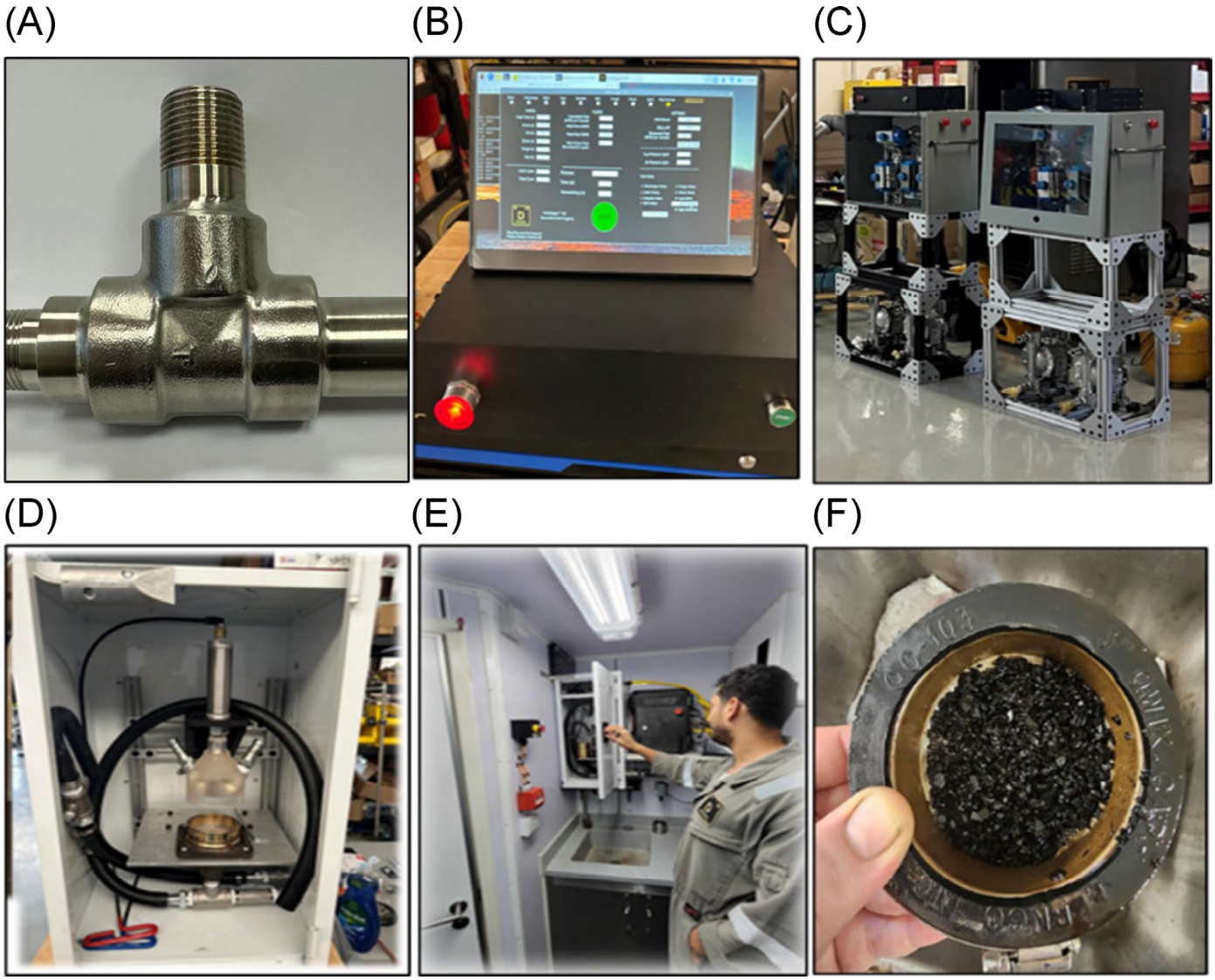

Figure 6. Automated sample collection system. (A) Extraction system in possum belly: water or diesel is used for transport and cleaning. Diesel dilution rates are coordinated with the mud engineer daily. (B) Diversified software & human machine interface (HMI). (C) Pumps and valve assembly. (D) Sample collection device. (E) Inside Unit view. (F) 20–30 grams of sample in collection cup.

feldspars, suggesting clay-rich sediments or weathered feldspar. K indicates the presence of feldspathic sandstones or shales due to its association with feldspars and mica. Fe, found in minerals such as hematite and magnetite, signals the presence of iron-bearing detrital minerals and secondary oxides. Ti and Zr are associated with heavy minerals like ilmenite, rutile, and zircon, which are resistant to weathering and indicative of detrital facies. Rb, often found in potassium-bearing minerals, reflects the contribution of feldspar and mica to the sediment. Analyzing the concentrations of these elements helps geoscientists identify detrital facies, providing insights into the sediments' provenance, transport history, and depositional environment.

Anoxic facies are sedimentary environments with little to no oxygen, leading to preserving organic matter and accumulating specific elements. Key indicators of anoxic conditions include high S and Fe concentrations, often present as iron sulfide minerals like pyrite. Elements such as Mo and U are enriched in anoxic facies because they precipitate under reducing conditions and remain soluble in oxygenated water. V and Ni are also commonly found in anoxic environments due to their association with organic matter and sulfide minerals. High total organic carbon (TOC) is a hallmark of these facies, as the lack of oxygen prevents organic matter decomposition, allowing it to accumulate. These geochemical signatures help identify anoxic facies, providing insights into past environmental conditions and highlighting potential source rocks for hydrocarbons (Ratcliffe et al., 2004).

Clustering complements PCA by grouping the PCA–transformed data into clusters, each representing samples with similar geochemical characteristics. Based on their geochemical signatures, these clusters correspond to different depositional environments. Geological interpretation of these clusters helps match them to specific environments, such as anoxic marine basins or fluvial settings, based on the elemental composition.

These chemostratigraphic zonations were plotted with the new wells in this study to categorize the chemostratigraphic variation along the vertical and lateral.

To better understand the relationship between chemostratigraphic units and chemofacies using the unsupervised approach

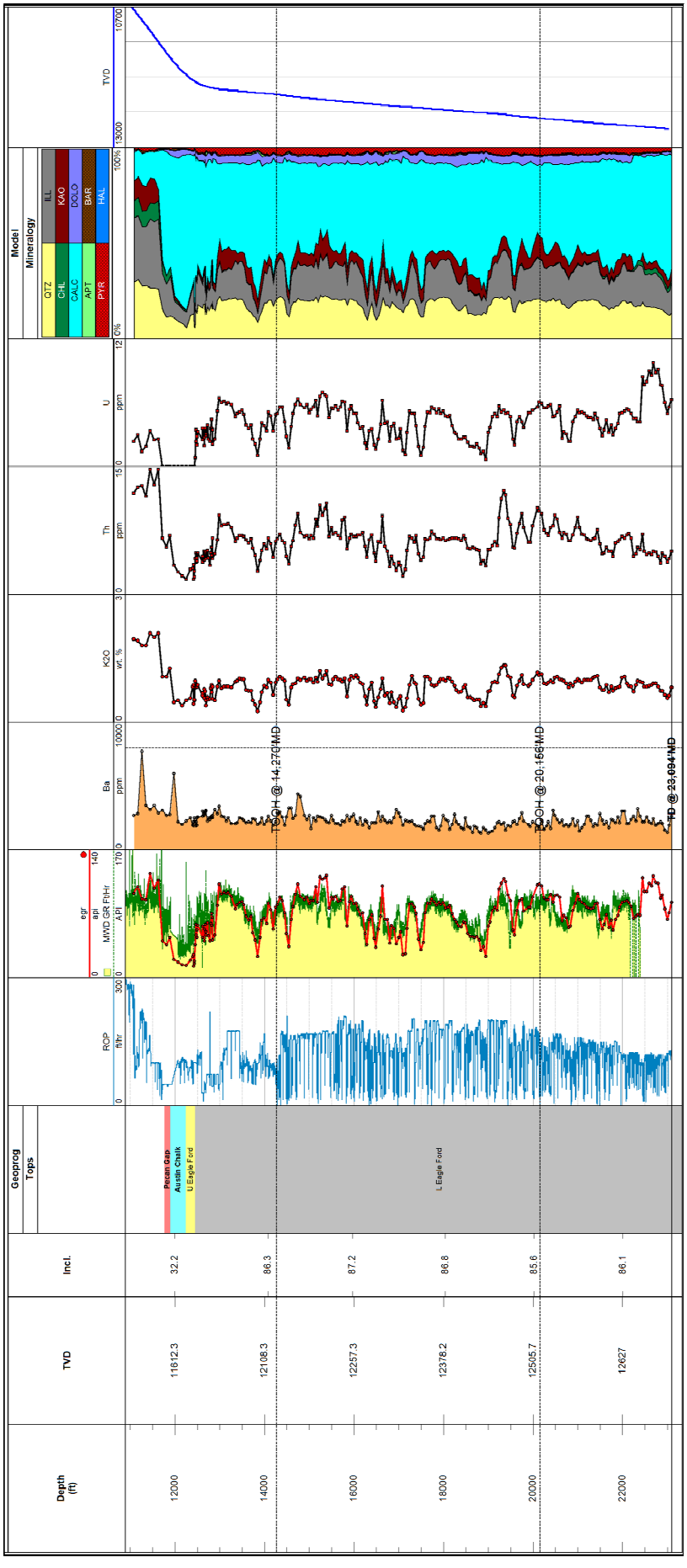

Figure 7. XRF quality assurance/quality control (QA/QC) panel displaying fepth (track 1); true vertical depth (track 2); inclination (track 3); Geoprog (geochemical progression) tops (track 4); rate of penetration (ROP) (track 5); EGR and MWD GR (track 6); Ba concentration in ppm (track 6); K_2O (wt.%), Th (ppm), and U (ppm) (tracks 8–10); mineralogical model (track 11); and true vertical depth curve (track 12). EGR compared to MWD GR correlates well indicating a high level of cuttings' representativity and Ba contamination levels are less than 10,000 ppm.

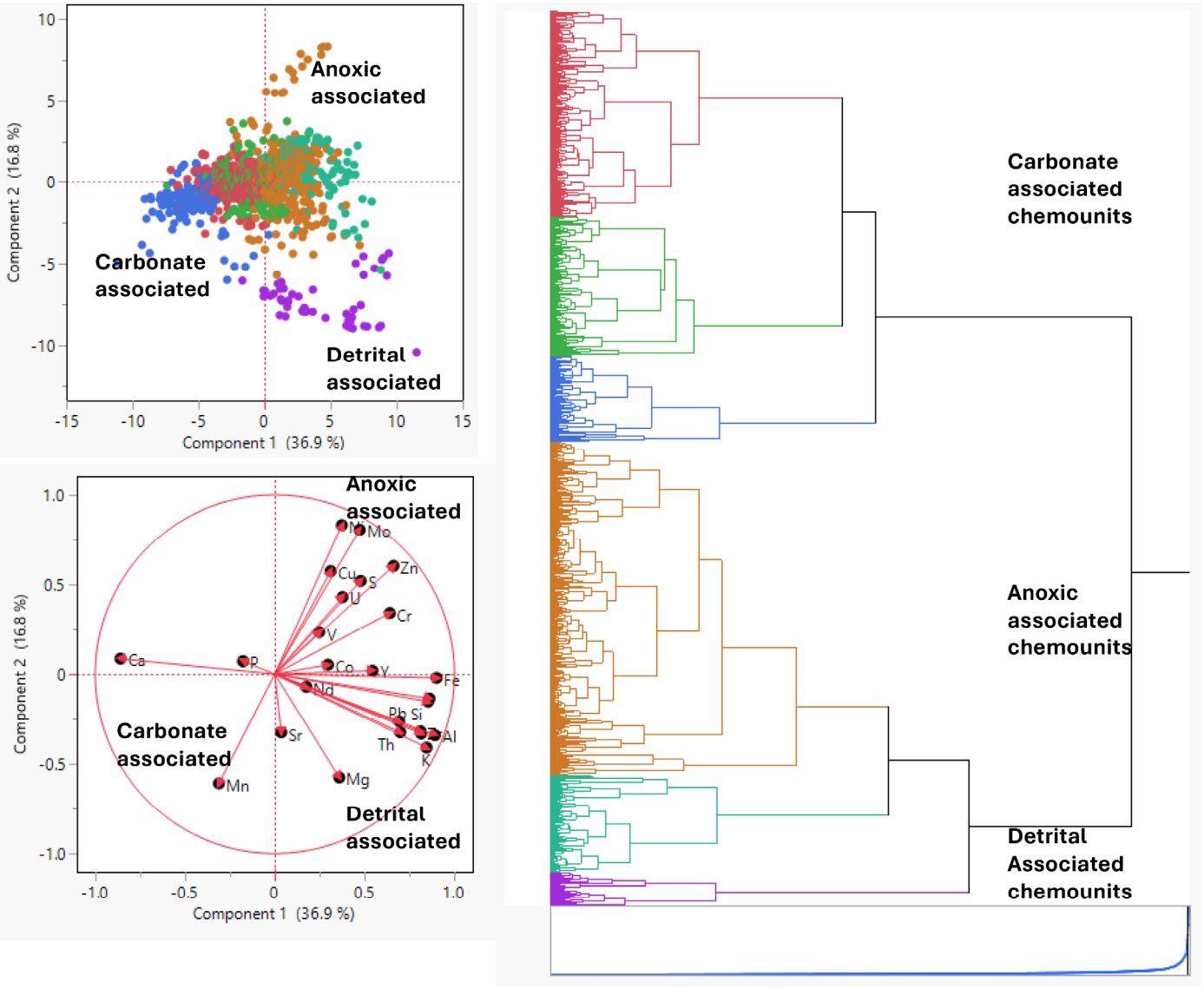

Figure 8. Principal component analysis (PCA) and cluster analysis were performed in 30+ wells in southeastern Texas. The image displayed the element and facies association of each chemounit.

(PCA), a supervised technique—discriminant function analysis (DFA)—was applied. DFA is a statistical procedure that classifies unknown individuals and estimates the probability of their membership in a specific group (such as chemounits) based on predictor variables (Klecka, 1980). The next phase involved training a model that used the chemostratigraphic units obtained and interpreted in the prior step to label each stratigraphic and chemically distinct stratigraphic horizons (9). To validate the model, 30% of the datasets were set aside. The validation process revealed that 8.07% of these data points were misclassified. Despite this, the overall accuracy of the model's predictions was considered highly suitable for real-time data labeling. This conclusion was based on the model's ability to accurately determine the chemical stratigraphic position compared to offset wells' data. The low misclassification rate indicates that the model is reliable and effective for real-time geological interpretation and decision-making.

Five chemostratigraphic units were identified in the dataset, detailing levels of anoxia, carbonate, and detrital components. These units were used to enhance wellbore placement and reservoir contact. (Fig. 9).

DATA AND RESULTS

The following example illustrates how the discriminant function analysis model was applied to inform geosteering decisions and optimize reservoir contact. Despite the high structural and geological complexity level, including multiple faults being transected, the model successfully utilized the data set to maintain wellbore positioning within the desired zone, ensuring maximum reservoir contact.

This modeling approach involved two distinct levels (Fig. 10). The first model was used to differentiate between the Austin Chalk and the Eagle Ford formations. Once the Eagle Ford was identified, a second, more detailed model was employed to further subdivide the Eagle Ford into discrete chemostratigraphic units, packages, and horizons. This multi-level modeling strategy allowed for precise stratigraphic identification, even in complex geological settings, enhancing the ability to stay in the zone and optimize hydrocarbon recovery.

Surface GR measurements derived from XRF analysis of drill cuttings were shown to complement or, in some cases, replace downhole GR measurements when the downhole tool

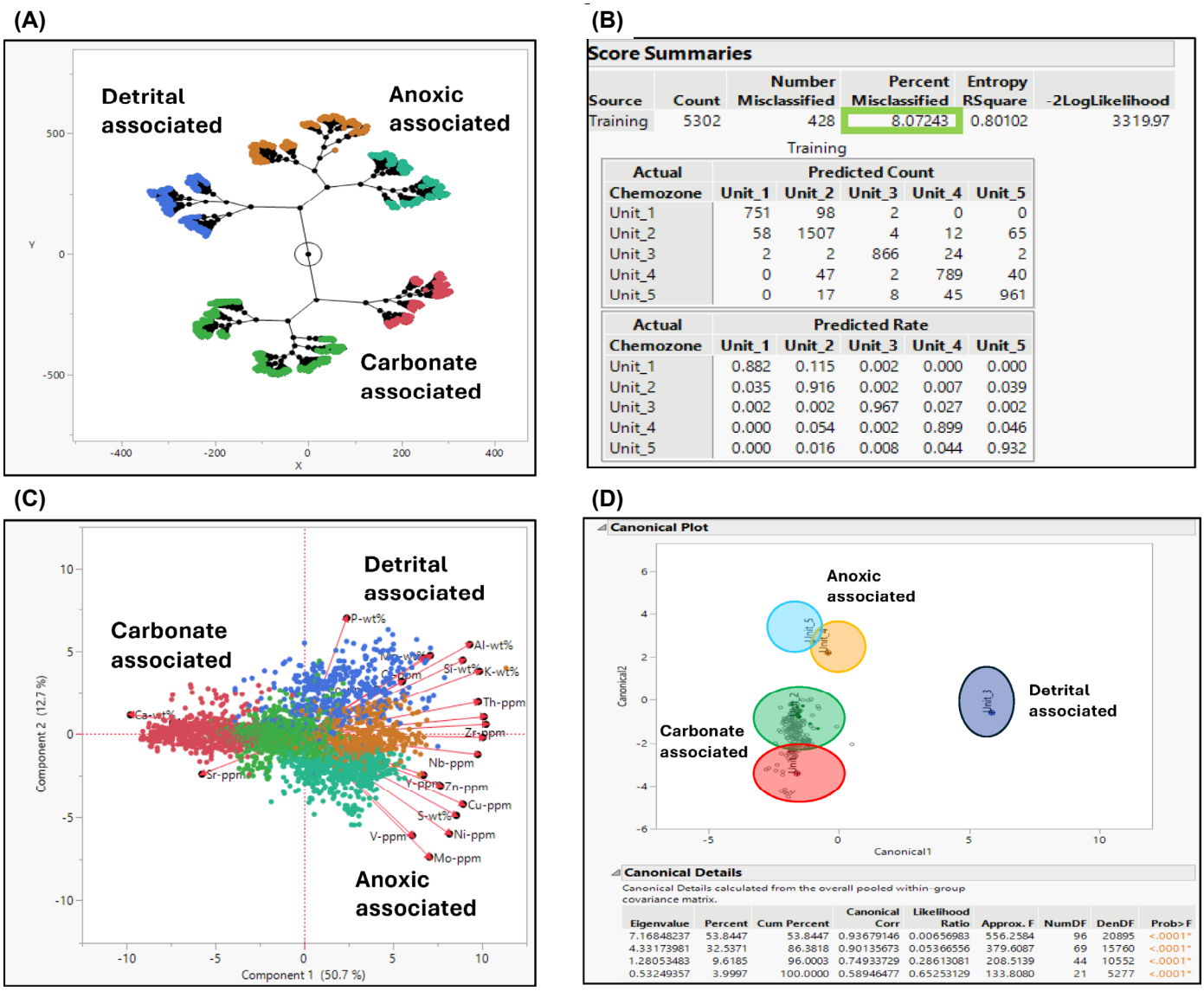

Figure 9. Discriminant function analysis (DFA) model generated using PCA and clustering results as training data from over 30 wells (Eagle Ford case study). (A) Constellation plot showing elemental associations along with chemozonations. (B) Score summary and confusion matrices displaying the number and percentage of correctly and incorrectly classified cases. (C) PCA highlighting elements associated with detrital, carbonate, and anoxic proxies. (D) Canonical plot illustrating how formations with similar elemental suites can be effectively differentiated.

failed. For example, as shown in Figure 11, the downhole GR tool failed towards the toe of the well , likely due to encountering a hard phosphate bed prior as can be seen in the second to last track to the right. The last section of the well was drilled to TD using the Robologger™ XRF SMWD measurements.

Geological insights include identifying depositional environments using several ratios and anoxic proxies mentioned previously, such as Ni/Mo and Zn/Mo, indicators of redox conditions, and sediment provenance during deposition. Organic-rich layers have notably increased the previously mentioned proxies and have been useful for hydrocarbon exploration. A general trend was noted, with an increase in anoxia from Dimmit County to Karnes County using the paleoredox-sensitive trace elements (Fig. 12). These changes in organic content helped support petrophysical log interpretations, ultimately leading to reserve adds and improved estimated ultimate recovery (EUR) calculations.

Changes in elemental compositions help delineate different sedimentary facies, such as shifts from clay-rich to siliceous or sandy sediments. These changes indicate variations in depositional energy and proximity to sediment sources, providing insights into the geological history and helping to identify potential reservoir zones. Key elemental ratios improved the understanding of subsurface geology, optimizing landing zones and geosteering operations. See the examples below, including identifying ash beds (Fig. 13), understanding caving origins (Fig. 14), and displaying wellbore instability (Fig. 15).

ASH BEDS IN THE LOWER EAGLE FORD

Ash beds are common in Eagle Ford (Donovan et al., 2010). Figure 13 illustrates the identification of volcanic ash layers and heavy elements within the LEF target using GR, EGR, and DFA models. The GR and EGR profiles on the left show variations that indicate changes in lithology, with peaks corresponding to higher concentrations of radioactive elements. The central DFA model track differentiates various lithological

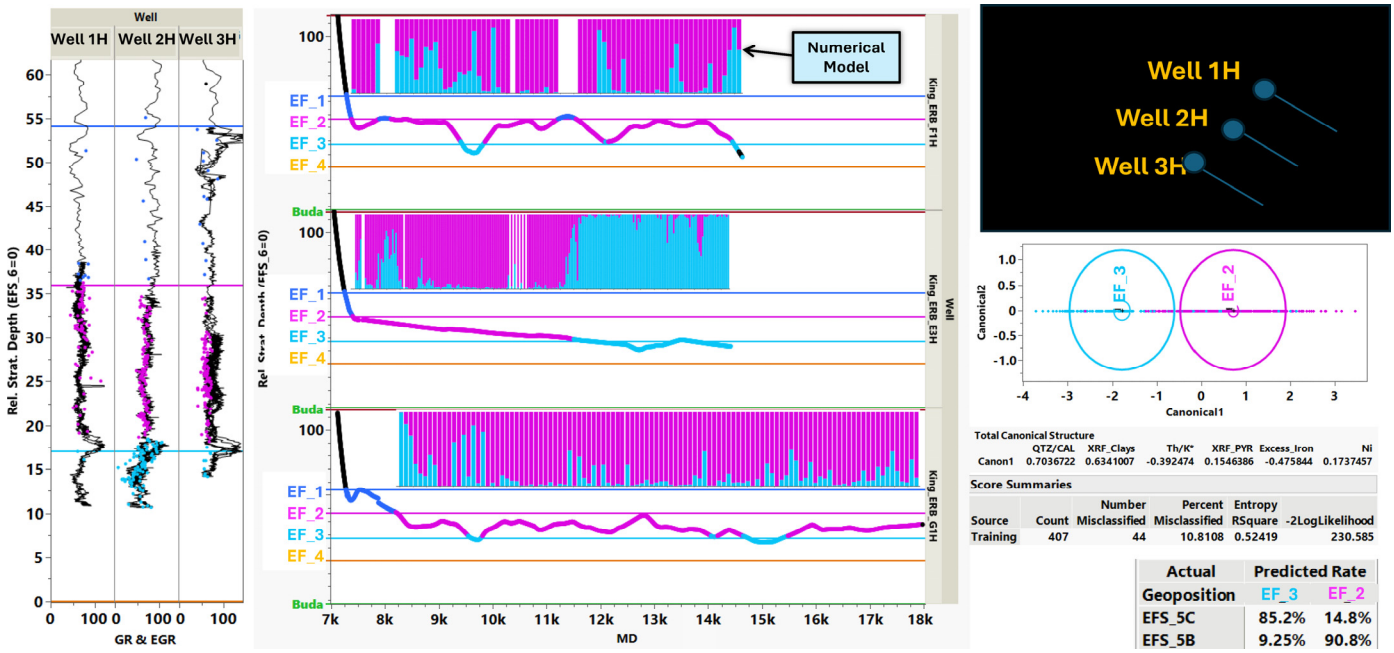

Figure 10. Application of DFA for geosteering in complex geological settings.

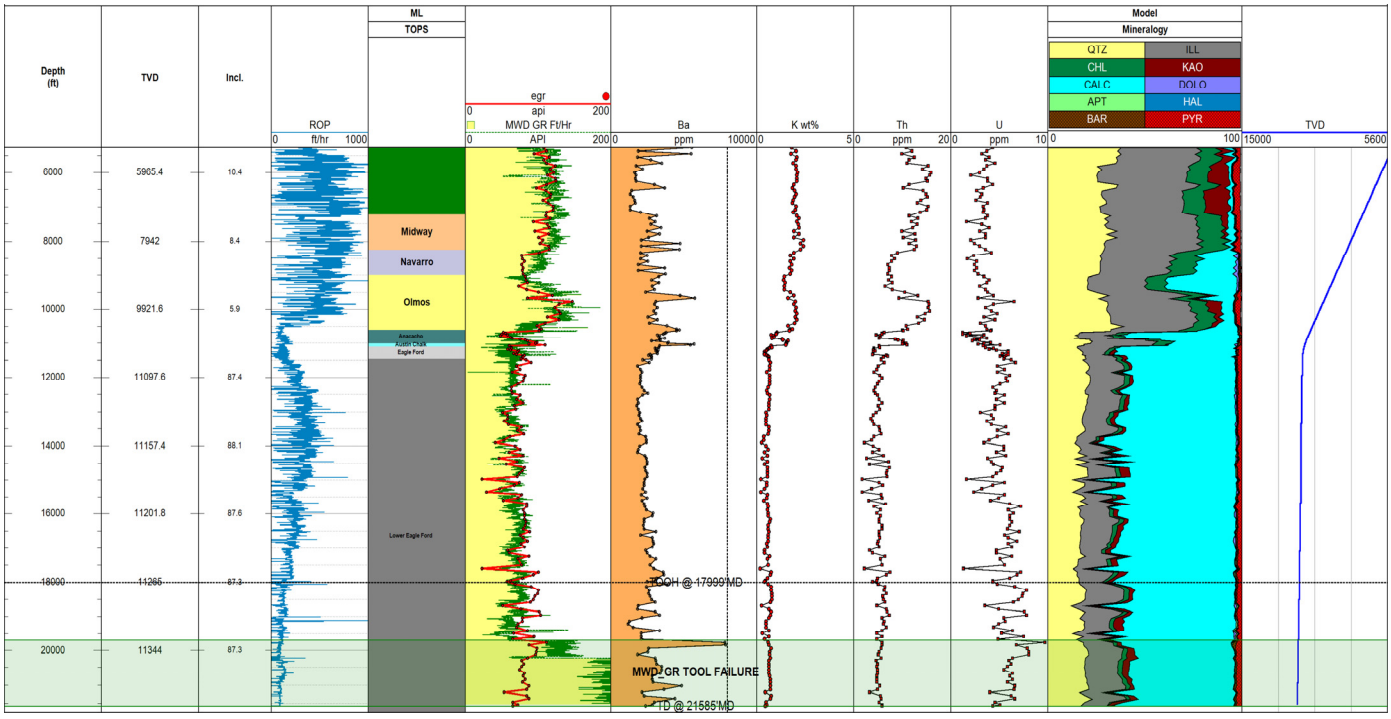

Figure 11. Example of reducing non-productive tripping time associated with MWD tool failure. The operator drilled ahead with the EGR and elemental data.

units, including volcanic ash layers, based on their geochemical signatures. The right panel's depth profile, with a green-to-red gradient, highlights zones of high heavy element and volcanic ash concentrations, pointing to ash beds. Fluorescence images confirm these ash layers, providing visual evidence. The "LEF target" zone is a key area of interest, enriched with volcanic ash and heavy elements, essential for understanding the depositional environment and assessing hydrocarbon potential in the Eagle Ford formation. The ability to measure the presence of ash beds using XRF data from drill cuttings was used as an active geosteering tool to avoid zones associated with drilling dysfunction.

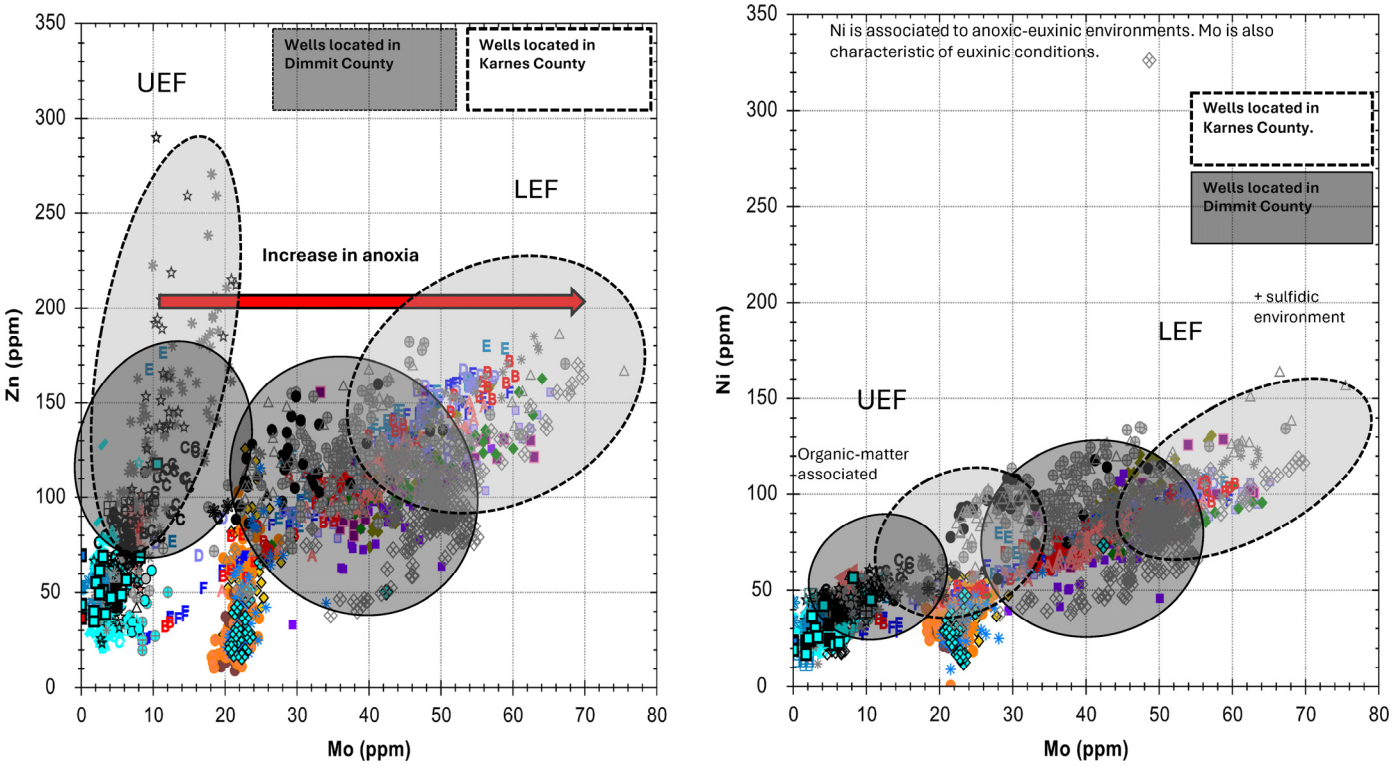

Figure 12. Zn/Mo and Ni/Mo plots displaying an increase in anoxia from Dimmit County to Karnes County using paleoredox proxies from inorganic elements.

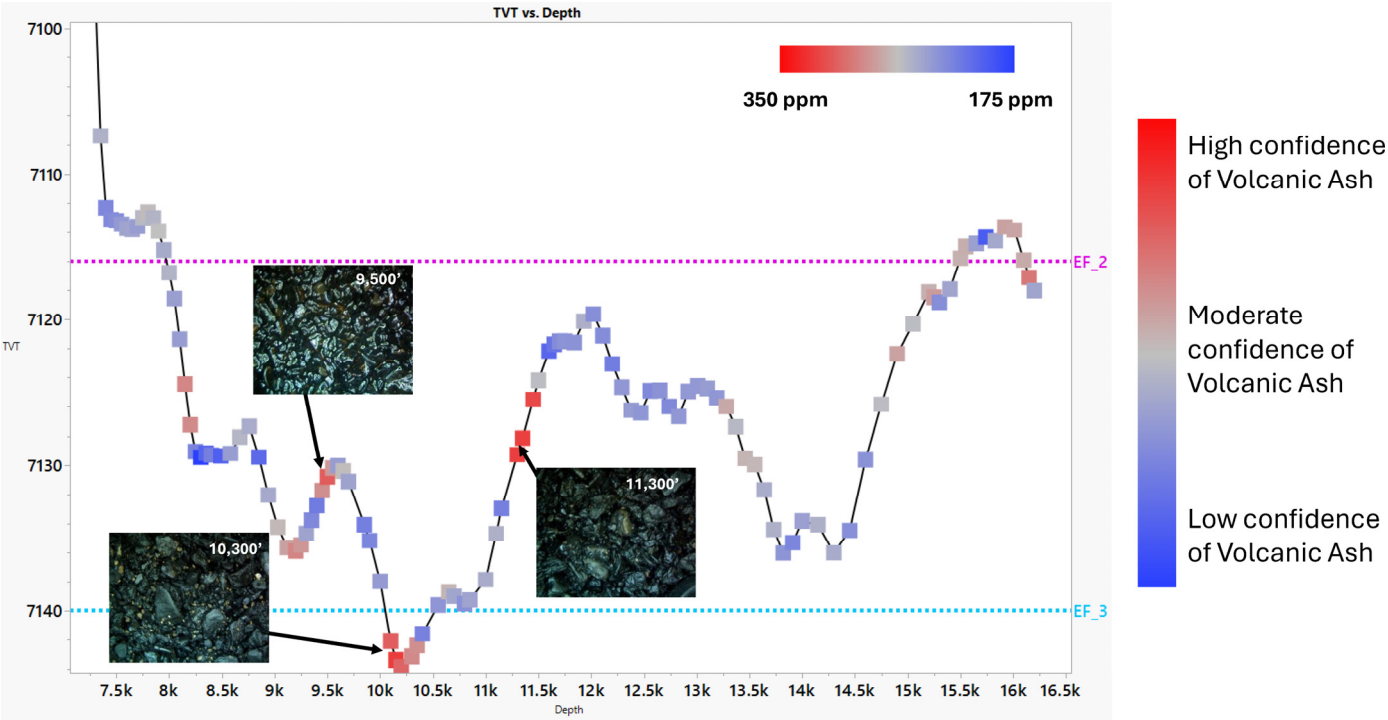

Figure 13. Identification of volcanic ash layers and heavy elements in the LEF target.

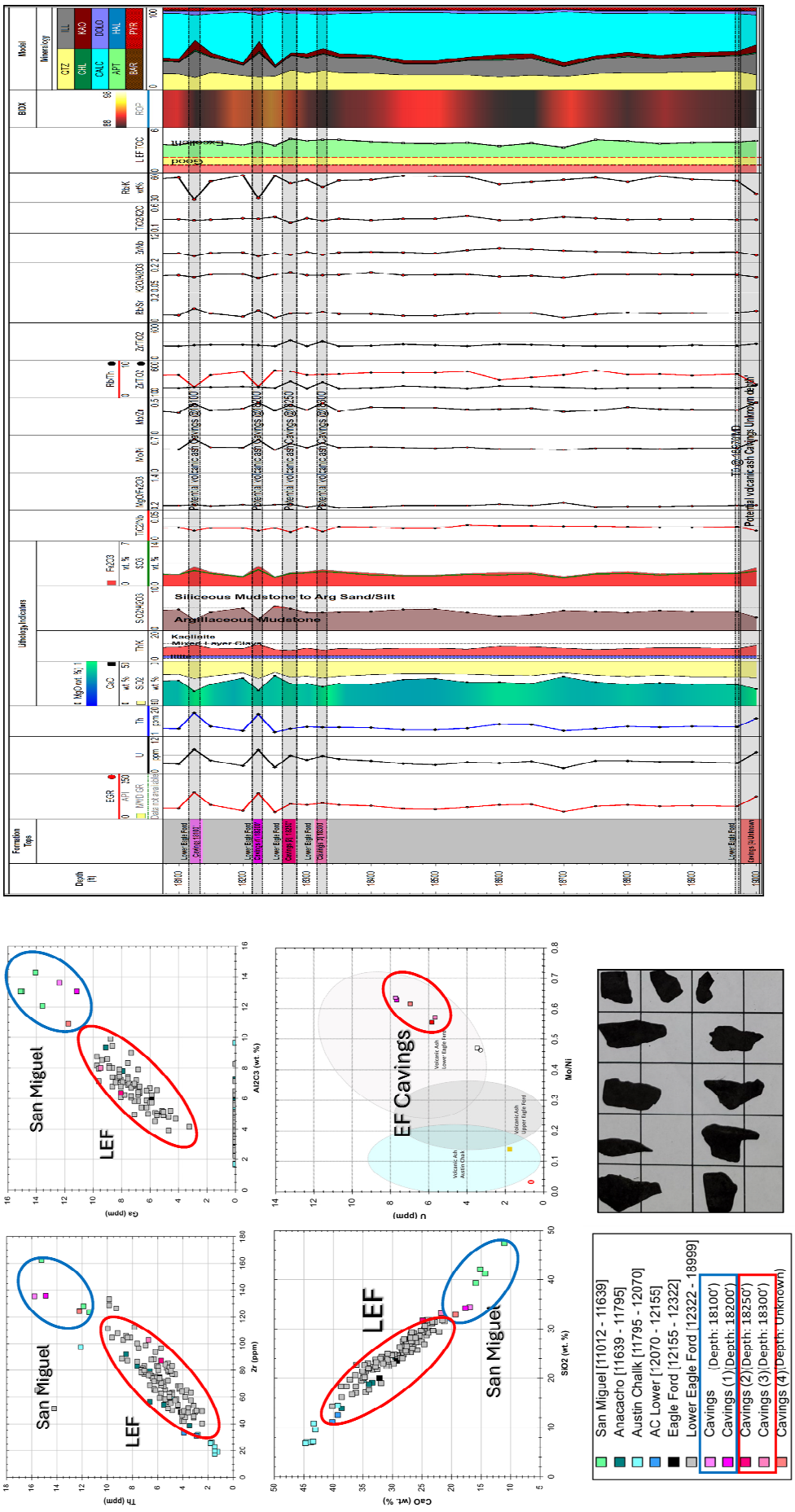

Figure 14. Identification of LEF cavings using cross-plots and well log data.

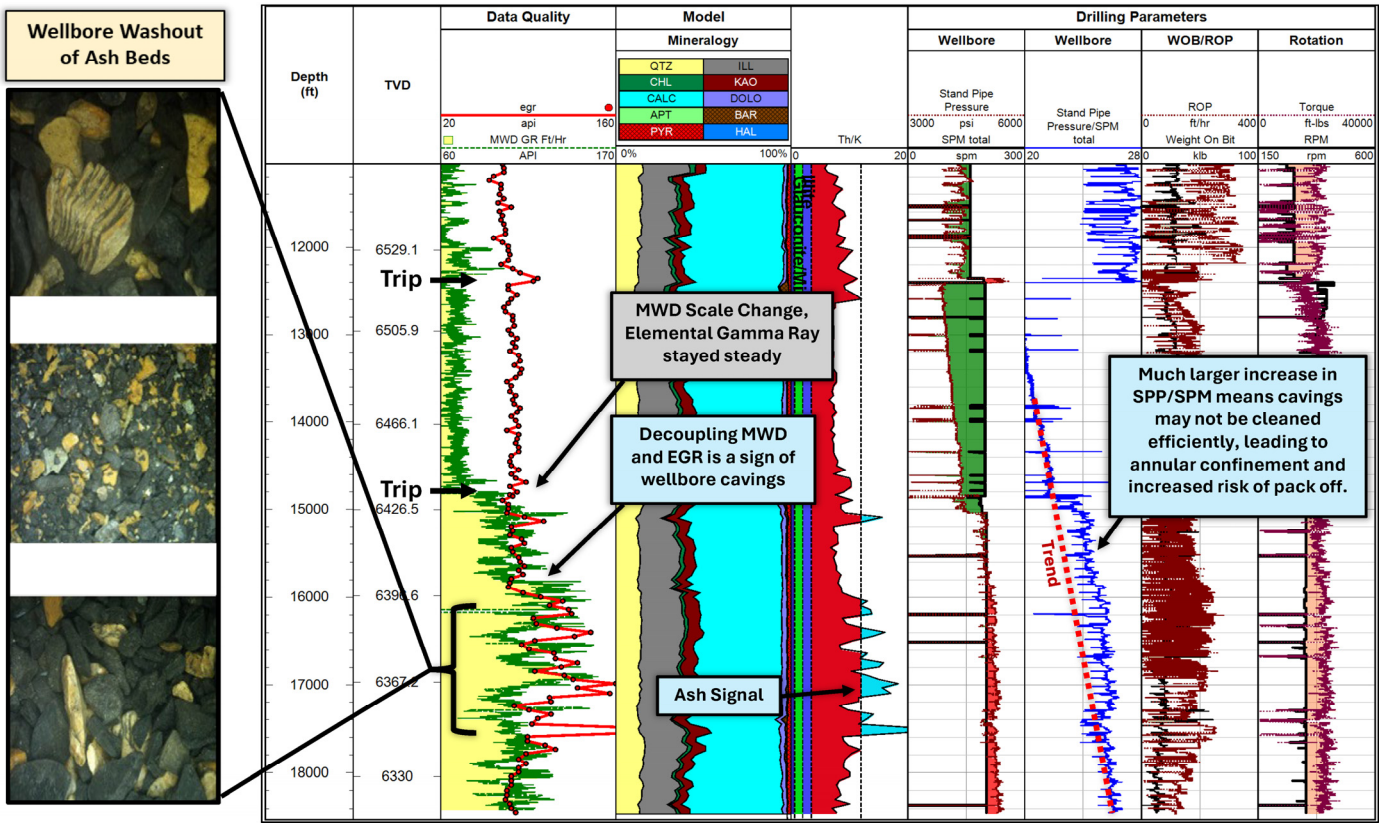

Figure 15. Wellbore washout and ash bed detection using elemental gamma ray (EGR) and MWD data mitigating cavings and pack off using drilling parameters. Panel displaying depth (track 1); true vertical depth (track 2); data quality (EGR vs. MWD GR, track 4); Th/K (track 5). Drilling parameters panel: standpipe pressure (SPP) and SPM total (track 6); weight on bit (WOB)/rate of penetration (ROP track 7); and torque and RPM (track 8).

WELLBORE CAVINGS DETECTION AND HOLE STABILITY

The decoupling of MWD GR with EGR can effectively indicate the presence of wellbore cavings or washout of ash beds. It is crucial to integrate drilling and geological indicators to ensure wellbore stability. Although mud loggers are typically responsible for identifying cavings, pinpointing the source visually can be challenging. However, the high-resolution elemental data in the subsurface allows using elemental binaries plots, PCA, and DFA to establish a direct fingerprint of the elemental data in specific formations, enabling the identification of cavings when present (Fig. 14). Identifying the source of cavings was critical in enhancing drilling operations by enabling targeted improvements in mud weight and strategic casing placement. Operators could adjust mud weights to stabilize the wellbore and prevent excessive cavings by pinpointing unstable zones. Throughout drilling multiple wells, this data-driven approach allowed for the optimization of well placement, steering wells away from zones with higher instability risks. As a result, wells were drilled with significantly reduced NPT caused by caving influxes and wellbore instability, leading to more efficient and cost-effective drilling operations. This proactive strategy minimized drilling complications and enhanced overall well integrity and safety.

Figure 15 compares MWD GR and EGR, pivotal in accurately representing in-depth cuttings. Inadequately cleaned wellbores following caving events or wellbore washout of ash beds can lead to stuck pipes and pack-off. This example shows increased standpipe pressure (SPP, wellbore pressure) versus strokes per minute (SPM, mud pump rate). This increase can be a helpful indicator of wellbore cleaning efficiency. A larger increase in SPP/SPM suggests that cavings may not have been efficiently removed, leading to annular confinement and an increased risk of pack-off. Drilling parameters and target horizons were modified to mitigate the pack-off and poor hole-cleaning issues.

In other examples, we have seen how an increase in phosphate can cause the deflection of drill bits and resultant slide drilling to reposition the wellbore in the target. The Paleocene-Eocene Thermal Maximum (PETM) was a significant global warming event approximately 56 million years ago. It was characterized by a rapid temperature increase associated with extensive carbon released into the atmosphere. This event profoundly impacted the Earth's climate, ocean chemistry, and ecosystems, leading to mass extinctions and significant changes in sedimentation patterns.

In the Eagle Ford Shale context, the PETM and similar periods of extreme climate change are often linked with an increase in phosphate levels in the geological record. Phosphate-rich layers in the Eagle Ford can indicate anoxic or euxinic conditions, where low oxygen levels in the water column led to preserving organic material and accumulating phosphates. These conditions are commonly associated with periods of high biological productivity followed by mass extinction events, as the increase in temperature and carbon dioxide levels disrupt marine ecosystems. (Erba et al., 2010; Stüben et al., 2005).

Phosphate-rich beds, such as those associated with the PETM and similar events in the Eagle Ford Shale, can be hard and have significant implications for drilling and completion operations. Phosphate beds tend to be relatively hard compared to surrounding sedimentary layers. The hardness results from the accumulation and diagenesis of phosphate minerals, which often

form dense, consolidated rocks. In the Eagle Ford Shale context, phosphate layers can form due to prolonged periods of low sedimentation rates and high biological productivity, leading to the concentration of phosphate minerals. Hard phosphate beds can cause increased wear and tear on drill bits, necessitating more frequent bit replacements and slowing drilling progress. This increases operational costs and downtime. The hardness of these beds can significantly reduce the penetration rate during drilling. Operators may need to adjust drilling parameters, such as weight on bit and rotational speed, to optimize drilling through these hard layers. The interface between hard phosphate beds and softer surrounding sediments can lead to differential stresses that may cause wellbore stability issues. This can result in borehole enlargement or collapse, complicating the drilling process.

The hardness and brittleness of phosphate-rich layers can influence how hydraulic fractures propagate. These beds might act as barriers to fracture growth, potentially limiting the effective drainage area of a well. During the completion phase, the hardness of phosphate beds can pose challenges for perforation. Higher energy charges may be required to perforate these layers effectively, and achieving consistent hole size can be difficult. The presence of hard, phosphate-rich layers can affect drilling efficiency and the placement and distribution of proppant during hydraulic fracturing. Ensuring adequate proppant penetration into these beds can be challenging, impacting the effectiveness of the fracture treatment.

Figure 14 illustrates the identification and characterization of the LEF using elemental data and cross-plots (left panel), along with a stratigraphic column and elemental profiles (right panel). The cross-plots show distinct geochemical signatures that indicate the presence of the LEF, highlighted by the green circles. These plots use elemental ratios such as aluminum oxide (Al_2O_3), phosphorus pentoxide (P_2O_5), U, and Ba to differentiate the LEF from other formations.

The stratigraphic column on the right provides a detailed view of the well log, showing depth (ft), true vertical depth (TVD), and inclination (Incl.). The column identifies key formations, including the Wilcox, Midway, Navarro, Olmos, and the targeted LEF. EGR and MWD GR profiles are plotted alongside other elemental concentrations (e.g., K, Th, and U), which confirm the geochemical indicators of the LEF.

The image of cavings samples (bottom left) visually confirms the geological interpretation, providing a physical basis for the identified geochemical signatures. These combined methods demonstrate the effective use of geochemical and visual data to identify wellbore stability and its origins. Identifying the sources of cavings was important for improving drilling operations, as it allowed for precise adjustments in mud weight and strategic casing placement. By pinpointing specific zones susceptible to instability, operators could fine-tune mud weights to stabilize the wellbore and reduce excessive cavings. This data-driven approach, applied across multiple wells, enabled optimal well placement by steering clear of areas with high instability risks. Consequently, wells experienced significantly less NPT due to reduced caving events and enhanced wellbore stability, resulting in more efficient and cost-effective drilling operations. This proactive strategy minimized drilling challenges and improved overall well integrity and safety.

Figure 15 illustrates the challenges associated with drilling through ash beds, as evidenced by wellbore washouts (left panel) and discrepancies between MWD GR and EGR data. The ash beds are characterized by a distinct ash signal (middle panel), where MWD and EGR decouple after entering the ash layer. This decoupling indicates a change in formation properties and highlights the limitations of MWD tools in accurately detecting ash beds. The EGR remains steady, providing a reliable signal through these challenging zones.

The drilling parameters (right panel) show significant increases in SPP and SPM during these intervals, indicating potential difficulties in efficiently cleaning cavings from the wellbore. This can lead to annular confinement, increasing the risk of pack-off and other wellbore stability issues. The observed trips highlight points where wellbore washouts occurred due to ash bed instability, underscoring the importance of accurately detecting and managing ash beds to maintain wellbore integrity and optimize drilling operations.

SAFETY

Over the two-year project, spanning operations at five drill sites and totaling 72,000 person-hours of work, there were zero safety incidents: no fatalities, no lost time incidents, no medical treatments beyond first aid, no first aid incidents, and no near misses, with only two at-risk behaviors observed (Fig. 16). This exemplary safety record proves that the automated sample collection system significantly reduced safety risks associated with slips, trips, and falls. Anecdotally, the authors visited the drill sites and observed high receptivity and satisfaction among the mud loggers, as the system provided a much cleaner and calmer work environment. This allowed personnel to focus on critical thinking and value-added tasks, significantly improving the retention rate of the loggers. Enhanced crew stability also reduced potential HSE risks, particularly those associated with new hires unfamiliar with the hazardous environment.

CONCLUSIONS

The innovative use of XRF and laser analysis of drill cuttings, combined with robotic automation for sample collection, offers a reliable and cost-effective alternative to traditional downhole measurements in the geologically complex Eagle Ford Shale. This approach reduces operational costs, enhances drilling efficiency, and significantly improves safety by reducing human exposure to hazardous conditions. This method's detailed geochemical insights allow for better well placement and optimized geosteering operations, directly contributing to increased reservoir contact and hydrocarbon recovery.

The DFA model proved instrumental in maintaining optimal wellbore positioning within the targeted reservoir zone, even in geologically complex areas with multiple faults. The dual-level modeling approach, differentiating between formations and further subdividing them into detailed chemostratigraphic units, enabled precise stratigraphic identification. This method enhanced hydrocarbon recovery by optimizing well placement.

In scenarios where downhole GR tools failed, surface GR measurements derived from XRF analysis successfully complemented or replaced these tools. This approach reduced non-productive tripping time and ensured continuous drilling operations, particularly in challenging geological conditions such as hard phosphate beds.

Using elemental ratios, such as the anoxic proxies, provided valuable insights into depositional environments and redox conditions. These proxies allowed for identifying organic-rich layers, contributing to a better understanding of hydrocarbon potential and supporting petrophysical log interpretations. The trend of increasing anoxia from Dimmit County to Karnes County highlighted the varying organic content across regions, leading to improved reserve calculations.

The ability to detect volcanic ash layers and wellbore cavings using high-resolution elemental data and DFA models was crucial in optimizing drilling operations. By identifying ash beds and their impact on wellbore stability, the approach enabled proactive adjustments in drilling parameters, reducing risks of stuck pipes and pack-offs.

Due to their hardness, phosphate-rich beds, often associated with significant geological events like the PETM, presented drilling challenges. These layers necessitated careful adjustments in drilling parameters and highlighted the importance of under-

Figure 16. Safety statistics.

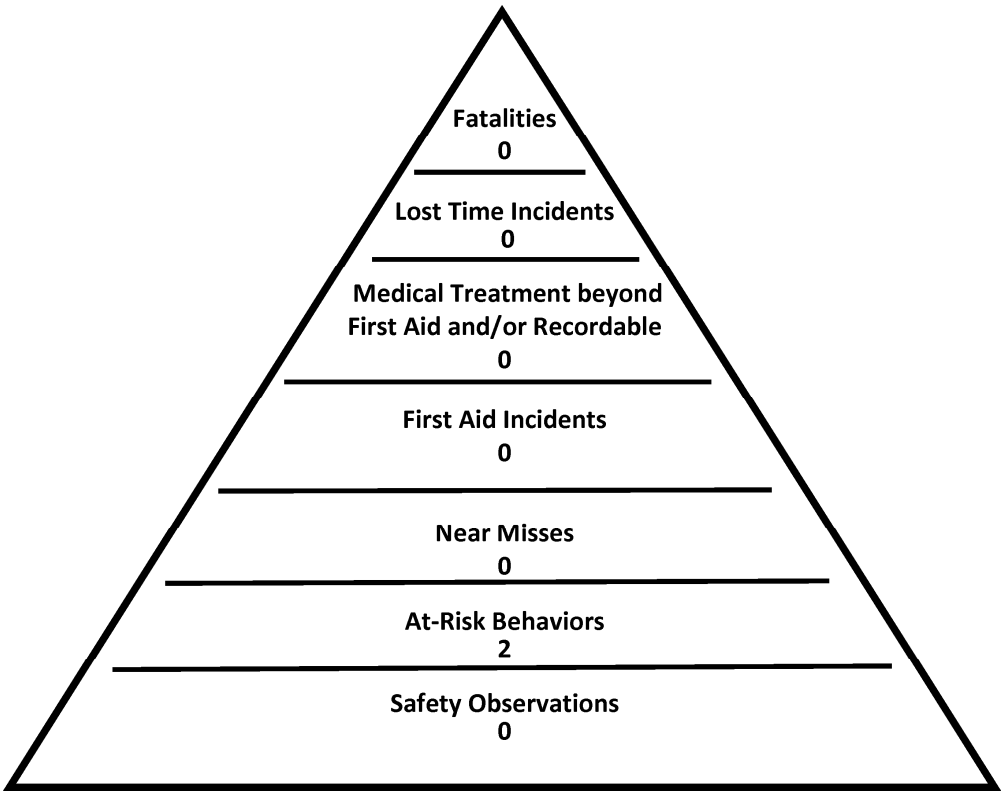

standing their impact on wellbore stability and hydraulic fracturing operations.

Integrating elemental data, cross-plots, and well log data allowed for precisely identifying zones prone to wellbore instability. This data-driven approach enabled targeted improvements in mud weight and strategic casing placement, significantly reducing NPT and enhancing overall well integrity and safety.

These conclusions demonstrate the effectiveness of advanced modeling techniques, elemental analysis, and proactive drilling strategies in optimizing reservoir contact, reducing operational risks, and enhancing overall hydrocarbon recovery.

ACKNOWLEDGMENTS

We want to acknowledge the contributions of the operations technical team involved in the XRF and laser analysis, the operators who provided access to well data, and the robotics engineers who facilitated the integration of automated sample collection.

REFERENCES CITED

Algeo, T. J., and J. B. Maynard, 2004, Trace-element behavior and redox facies in core shales of Upper Pennsylvanian Kansas-type cyclothems: Chemical Geology, v. 206, p. 289–318, <https://doi.org/10.1016/j.chemgeo.2003.12.009>.

Algeo, T. J., and N. Tribovillard, 2009, Environmental analysis of paleoceanographic systems based on molybdenum-uranium covariation: Chemical Geology, v. 268, p. 211–225, <https://doi.org/10.1016/j.chemgeo.2009.09.001>.

Amosu, A., 2015, An angular unconformity between the Woodbine and Eagle Ford formations in Delta, Hunt and Hopkins counties, Texas: Gulf Coast Association of Geological Societies Transactions, v. 65, p. 45–75.

Donovan, A. D., and T. S. Staerker, 2010, Sequence stratigraphy of the Eagle Ford (Boquillas) Formation in the subsurface of South Texas and outcrops of West Texas: American Association of Petroleum Geologists Bulletin, v. 94, p. 165–190, <https://doi.org/10.1306/06300909003>.

Donovan, A. D., T. S. Staerker, J. M. Spaw, and A. R. McInturff, 2015, The Austin Chalk and Eagle Ford Formations in the subsurface of Texas: A story of local tectonics and global sea-level change: American Association of Petroleum Geologists Bulletin, v. 99, p. 209–234, <https://doi.org/10.1306/09021413111>.

Ellis, D. V.. and J. M. Singer, 2007, Well logging for earth scientists, 2nd ed.: Springer Netherlands, 728 p.

Erba, E., C. Bottini, H. J. Weissert, and C. E. Keller, 2010, Calcareous nannoplankton response to surface-water acidification around Oceanic Anoxic Event 1a: Science, v. 329, p. 428–432, <https://doi.org/10.1126/science.1188886>.

Everitt, B. S., S. Landau, M. Leese, and D. Stahl, 2011, Cluster analysis, 5th ed.: Wiley, 330 p.

Hentz, T. F., and S. C. Ruppel, 2010, Regional stratigraphic and rock characteristics of the Eagle Ford Shale in its play area: Maverick Basin to East Texas Basin: American Association of Petroleum Geologists Search and Discovery Article 10325, 20 p., <https://www.searchanddiscovery.com/pdfz/documents/2011/10325hentz/ndx_hentz.pdf.html>.

Hild, E., and H. J. Brumsack, 1998, Major and minor element geochemistry of Lower Aptian sediments from the NW German Basin: Cretaceous Research, v. 19, p. 615–633, <https://doi.org/10.1006/cres.1998.0137>.

Jolliffe, I. T., 2002, Principal component analysis, 2nd ed.: Springer, 488 p.

Klecka, W. R., 1980, Discriminant analysis: Sage Publications, Quantitative Applications in the Social Sciences Series 19, 72 p.

Larson, T. E., J. E. Sivil, P. Periwal, and J. Melick, 2023, A machine-learning workflow to integrate high-resolution core-based facies into basin-scale stratigraphic models for the Wolfcamp and Third Bone Spring Sand, Delaware Basin: Interpretation, v. 11, no. 4, p. SC91–SC104, <https://doi.org/10.1190/INT-2023-0009.1>.

Liu, Z., Y. Zhang, and Y. Wu, 2017, Geochemical characteristics of the Eagle Ford Shale and implications for paleoenvironment and hydrocarbon potential: Marine and Petroleum Geology, v. 86, p. 1110–1122, <https://doi.org/10.1016/j.marpetgeo.2017.06.025>.

Railroad Commission of Texas, 2024, Eagle Ford Shale: <https://www.rrc.texas.gov/oil-and-gas/major-oil-and-gas-formations/eagle-ford-shale/>.

Ratcliffe, K. T., A. M. Wright, C. R. Hallsworth, A. C. Morton, B. A. Zaitlin, D. Potocki, and D. S. Wray, 2004, An example of alternative correlation techniques in a low-accommodation setting, non-marine hydrocarbon system: The (Lower Cretaceous) Mannville Basal Quartz succession of southern Alberta: American Association of Petroleum Geologists Bulletin, v. 88, p. 1419–1432, <https://doi.org/10.1306/05100402035>.

Reimann, C., P. Filzmoser, R. Garrett, and R. Duttor, 2011, Statistical data analysis explained: Applied environmental statistics with R: Wiley, 368 p.

Romero-Sarmiento, M. F., M. Rousselle, P. Faure, H. Wilkes, and X. Boespflug, 2014, Origin of organic matter in the Eagle Ford Formation (Texas): Evidence from geochemical data: International Journal of Coal Geology, v. 136, p. 1–12, <https://doi.org/10.1016/j.coal.2014.11.001>.

Stüben, D., U. Kramar, Z. Berner, and A. Eckardt, 2005, Phosphate-rich sediments from the Cretaceous-Tertiary boundary (Fish et al.): Palaeogeography, Palaeoclimatology, Palaeoecology, v. 224, p. 161–181, <https://doi.org/10.1016/j.palaeo.2005.03.054>.

Tinnin, B., and S. Darmaoen, 2016, Chemostratigraphic variability of the Eagle Ford Shale, South Texas: Insights into paleoredox and sedimentary facies changes, *in* J. A. Breyer, ed., The Eagle Ford Shale: A renaissance in U.S. oil production: American Association of Petroleum Geologists Memoir 110, p. 259–283.

Tribovillard, N., T. Algeo, T. W. Lyons, and A. Riboulleau, 2006, Trace metals as paleoredox and paleoproductivity proxies: An update: Chemical Geology, v. 232, p. 12–32, <https://doi.org/10.1016/j.chemgeo.2006.02.011>.

Workman, S. J., and G. M. Grammer, 2013, Integrating depositional facies and sequence stratigraphy in characterizing unconventional reservoirs: Eagle Ford Shale, South Texas: Gulf Coast Association of Geological Societies Transactions, v. 63, p. 473–508.